Determining directional emissivity : numerical estimation and experimental validation by using infrared thermography

Determining directional emissivity: numerical estimation and experimental validation by using infrared thermography

J. Peeters[a,*], B. Ribbens[a], J.J.J. Dirckx[c], G. Steenackers[a,b]

[a] *University of Antwerp, Op3Mech, Salesianenlaan 90, B-2660 Antwerp, Belgium. Tel.: +32-3-2051938*
[b] *Vrije Universiteit Brussel, Acoustics & Vibration Research Group, Pleinlaan 2, B-1050, Brussels, Belgium.*
[c] *University of Antwerp, Laboratory of Biomedical Physics, Groenenborgerlaan 171, B-2020 Antwerp, Belgium.*

Abstract

Little research has examined that inaccurate estimations of directional emissivity form a major challenge during both passive and active thermographic measurements. Especially with the increasing use of complex curved shapes and the growing precision of thermal cameras, these errors limit the accuracy of the thermal measurements. In this work we developed a technique to estimate the directional emissivity using updated numerical simulations. The reradiation on concave surfaces is examined by thermal imaging of a homogeneous heated curved metal and nylon test sample. We used finite element modelling to predict the reradiation of concave structures in order to calculate the parameters of an approximating formula for the emissivity dependent on the angle to the normal vector on each element. The differences between experimental and numerical results of the steel test sample are explained using electron microscopy imaging and the validation on different materials. The results suggest that it is possible to determine the errors of thermal imaging testing of complex shapes using a numerical model.

Keywords: thermal imaging, emissivity, finite element modelling, thermography, inverse problem

*Ing. Jeroen Peeters
Email address: jeroen.peeters2@uantwerpen.be (J. Peeters)
URL: www.op3mech.be (J. Peeters)

1. Introduction

Most thermographic non-destructive testing research is performed on flat test samples like flat bottom hole plates to improve thermographic post-processing techniques [1]. In general thermographic applications, structural health monitoring inspections are performed on complex shaped structures. With the use of complex geometrical surfaces, there are several parameters which influence the measured radiation, including self-radiation and the angular dependency of the emissivity [2]. Self-radiation is defined as the emittance which is emitted back to the object in the infrared spectral bandwidth. For active thermal inspections a variety of techniques exist which use signal delay measurements and phase images instead of intensity maps to filter the signal from the ambient conditions [1, 3, 4]. Most applications use IR imaging for passive investigations [3] where the history of preheating is unknown and the influence of emissivity, reflections and ambient conditions are an important aspect of the image evaluation. To predict correct temperature profiles of complex shaped structures it is therefore useful to have a predictive tool to calculate the nominal measured temperature offsets due to directional emissivity of the complex structure versus the real temperatures. Most influences of thermal noise on the measured temperatures, such as the influence of ambient reflections and the influence of sensor noise, could be reduced by the use of multiple view points. Furthermore, the directional emissivity which results in different measured temperature profiles of concave and convex surfaces can only be predicted analytically for simple geometries. The directional emissivity errors are geometry and view point dependent. Nowadays, structures become more and more complex shaped because of the extensive implementation of high-end composite materials. Due to the increase in accuracy of thermal cameras over the past ten years, the need arises to eliminate geometry-caused errors in order to be able to measure more precisely and deeper in structures. In the 1970's Kanayama already developed numerical models to describe the directional emittances for rough surfaces [5] theoretically using Fresnel's formula. Furthermore it is well known and broadly discussed that the roughness of a surface influences the emissivity [6]. In the early 1960's a numerical ray tracing technique was developed for V-shaped grooves [7, 8] which was further developed by Birkebak and Eckert [9] and Sacadura as shown in [6]. Besides, numerical simulations by finite element (FE) modelling of the directional emissivity on surfaces with random grooves were not considered sufficiently accurate in the 1990's [10]. Recent studies show that with increasing calculation power, the use of finite element modelling to numerically estimate multiple scatterers in three dimensions delivers reliable results [11]. In recent years, major steps were taken towards a better understanding of the directional behaviour of thermal emittance in laboratories [12, 6, 13, 14, 15, 16]. We continue this research by implementing these techniques in realistic structures and designing a technique with which the numerical model can be adapted to the realistic manufacturing conditions.

To estimate the influence of directional emissivity on temperature measurements for quality control, we developed a technique using numerical analysis to model the directional emissivity by updating the emissivity profile from experimental validation data. This paper proposes a methodology to evaluate the experimental directional emissivity with numerical simulation data. Therefore the paper starts with a theoretical overview of the directional

dependency of emissivity and the approximation methodologies. Next the experimental measurements of the directional emissivity for a simple concave and convex surface are described. We proceed with the description of the numerical model, followed by a discussion section where we validate the measurements of different samples, and we end with the conclusions.

2. Materials & Methods

Within this section we will first deliver some theoretical background of directional emissivity, then we will define the performed experimental measurements and finally we will describe the numerical modelling.

2.1. Theoretical background

The emissivity of a structure is dependent on multiple parameters such as the type of material, the surface roughness, the wavelength range and the angle between the camera and the structure [3, 1].

The cosine law of Lambert [1] Eq.(1) shows that the emitted radiation intensity (ΔT_p) has a maximum normal to the face angle and a minimum normal at larger angles δ, as can be seen in Figure 1:

$$\Delta T_p \sim \epsilon \frac{P\, cos(\delta)\, \Delta t)}{4\pi\, R^2 \rho\, C\, dz}\ (^{\circ}\mathrm{C}) \tag{1}$$

where R is the distance between the point source and the object (m), δ the angle between the normal to the surface and the incident ray (rad), P is the heating power (W), ρ the density (kg/m^3), Δt the thermal pulse length (s), dz the depth of penetration of the heating front (m), C the specific heat (J/kg $\cdot$ °C), and ϵ the directional emissivity. In reality the intensity distribution is far more complex than a Lambert radiator [3]. Most active thermography techniques make use of previously recorded thermograms (ERT) to compensate the radiation distribution for non-planar surfaces [1]. This technique, fully described in [1] has multiple drawbacks:

- Calibration recording before excitation is essential for each part and makes the technique very slow.
- A high-powered source is required of which only a fraction is used.
- The maximum workable workspace and distance are limited.
- Restricted to limited curvature as the cos(δ) is unknown.

By using an updated FE model it is possible to predict the thermal response of a complex curved structure by estimating the $cos(\delta)$ from the geometry data.

By the use of active thermography, the inspected object is heated by a heat source for a short time period. Due to direct emissivity, a certain part of the by itself emitted energy

will be reabsorbed again by the structure due to self-radiation. The amount of re-absorbed energy is dependent on the amount of radiation received from the emitting surface, as shown schematically in Figure 1 by the different sized arrows. In this figure, the blue solid arc represents a curved structure and the gradient arc represents the observed temperature distribution. For the comparison of thermography measurements with theoretical values it is essential to model this viewing angle dependent emissivity. Therefore we need to estimate the angle dependence of the emissivity by defining a custom function. Based on a general Lambertian function dependent of angle δ this function is built for a specific structure by iterative updating of a FE model in order to estimate the directional dependency weights using the Monte Carlo ray tracing routines. The temperature profile of the FE model is compared with the measured temperature profile of the experimental measurements.

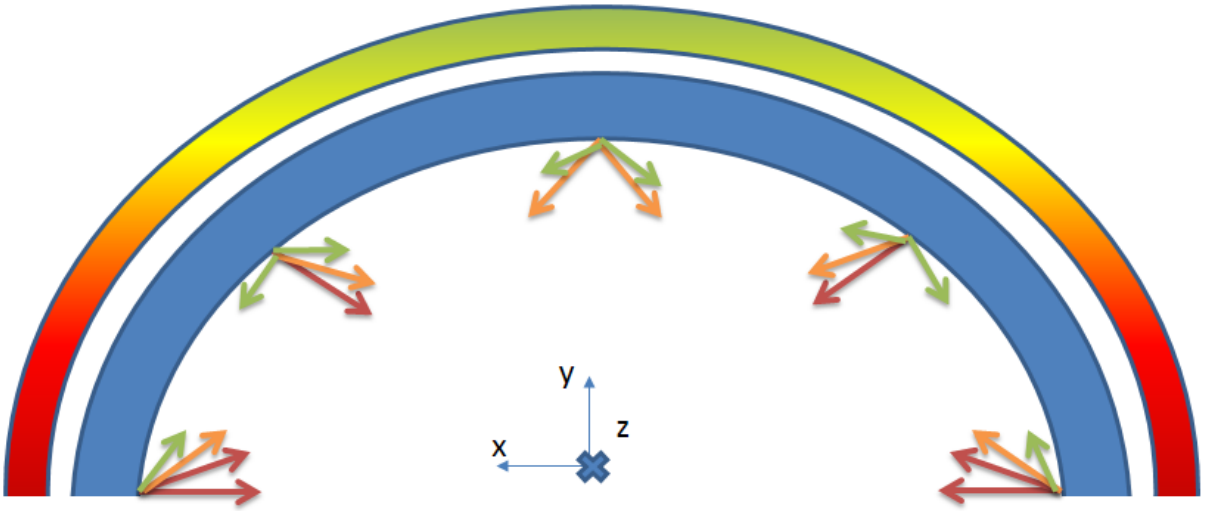

Figure 1: Schematic overview of the directional dependency of emissivity. The relative size of the directional emissivity factor for the reradiation of the concave surface is represented by the length and color of the arrows and an estimated temperature distribution along the concave surface is plotted above the solid tube section.

2.2. Experimental measurements

To investigate the self-radiation of concave structures, we homogeneously heated a steel and nylon tube section to a temperature above 40°C using a hot fluid medium on a homogeneous temperature and placing them vertically to deliver an equal convection flux over the full arc in an ambient atmosphere of 22°C. The tube section is placed in a thermal stable environment with homogeneous ambient reflections and has an elevated homogeneous temperature in advance, in contrast to the absorbing background walls. We expect that the surface temperature at the outer surface of the tube section delivers a horizontal profile with a constant temperature, as self-radiation is impossible at a convex surface. For the inside of the tube we expect a completely different profile as self-radiation influences the measurements of the concave surface. The directional emissivity of the concave surface is shown in Figure 2. In the concave measurement profile we found two

regions of remarkably high temperature measurements at the side of the concave surface. Note that the structure itself is globally 43°C Celsius but that the outer sides of the concave surface show a higher temperature due to self-reflectivity and self-radiation. The true material temperatures without reflection and self-radiation are measured from the convex side of the tube section. The experimental measurements were performed with a Xenics Gobi640 Gige-E microbolometric camera with 640×480 resolution with a NETD of 50 mK and a spectral range of 7-14 μm with negligible external radiation. The camera is placed in front of the tube section under three different angles which are averaged out for each geometrical point of the tube. The tube section is heated to a temperature between 40 and 50 °C which has its maximal spectral emission in the spectral range of the camera. As we know that the temperature of the surface is the same for each point at initial conditions (homogeneously heated), the only possible explanation for this measurement is the view-angle dependency of the emissivity as explained in [1, 3]. As the concave surface is subjected to self-radiation, the emitted radiation in directions with a large angle has less energy than the radiation normal to the face. This is graphically shown in Figure 1. To improve the emissivity and eliminate the influences of roughness and reflections, the surfaces of the steel tube are coated with an acrylic paint coating which improves the emissivity to an estimated emissivity of 0.9, providing a smooth absorbing surface.

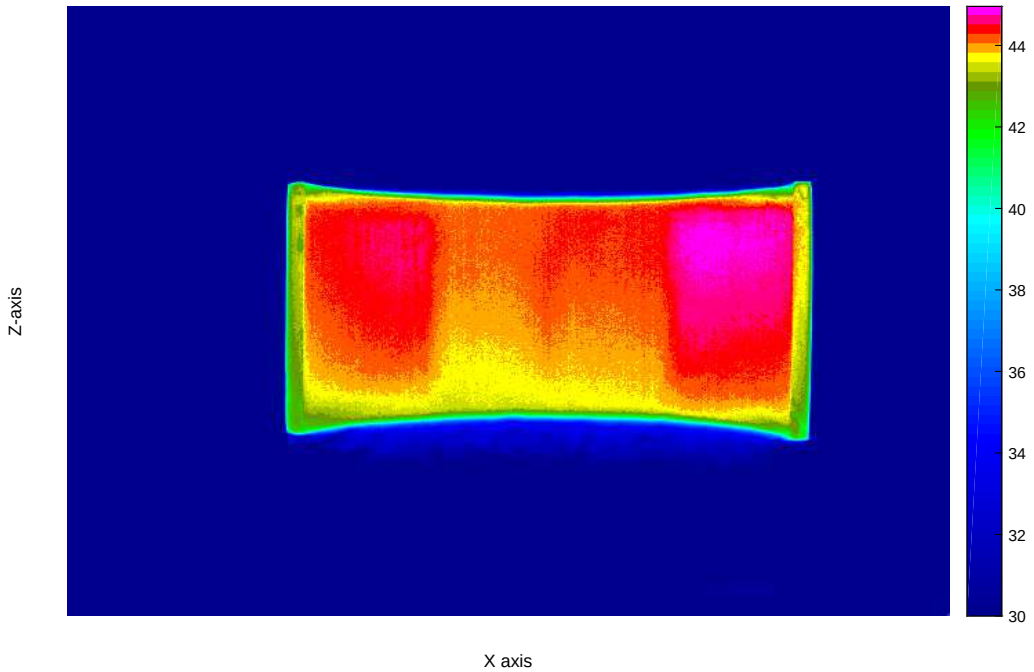

Figure 2: The measured temperature due to directional emissivity at the concave surface of a homogeneous heated surface at 43 °C viewing the ZX plane.

2.3. Numerical estimation

The numerical FE model of the directional emissivity is built with the Monte Carlo ray-tracing technique for radiating surfaces in the commercial Siemens NX 8.5 software. The Monte Carlo ray-tracing technique has already proven its success in the simulation of directional emissivity [17, 2]. We made use of a multi-layered 3D mesh of 4500 linear quad elements. The material properties are defined in Table 1. The directional emissivity is defined as an angular dependent thermo-optical property. This is formula-based according to equation Eq. (2) dependent of two unknown parameters.

The directional emissivity will be approximated with:

$$\varepsilon(\theta) = \max(\cos(\sqrt{\mathrm{P}_1}\theta + \mathrm{P}_2 * \pi), 0) \tag{2}$$

where P_1 and P_2 are the optimized parameters to reshape the cosine function during the iterative FE updating progress to fit the experimental model.

Table 1: Material properties FE model.

Optimization method	Tube	Coating
Material	Steel	Acrylic paint [18]
Density ρ (kg/m^3)	7 829	1 200
Thermal conductivity k (W/m $\cdot$ °C)	54.8-55.7 [$50 - 20\,°C$]	0.205
Specific heat capacity C_p (J/(kg $\cdot$ °C))	434	1 500

The solved numerical model can be described using the following equations Eq. (3-8) assuming a three dimensional heat flow with negligible external radiation.

The standard heat equation inside a solid material is defined by:

$$\frac{\partial T}{\partial t} = \alpha \left(\frac{\partial^2 T}{\partial x^2} + \frac{\partial^2 T}{\partial y^2} + \frac{\partial^2 T}{\partial z^2} \right) \tag{3}$$

where $\mathrm{T}_{\mathrm{init}}$ is the initial temperature:

$$T(x, y, z, t = 0) = T_{init};\ 0 < x < H;\ 0 < y < L;\ 0 < z < d; \tag{4}$$

Most boundary conditions are defined according to reference [19, 20] straightforwardly, only the boundary condition of the convex and concave surfaces should receive special attention.

The boundary condition of the convex surface:

$$-k\frac{\partial T}{\partial x} = -k\frac{\partial T}{\partial y} = h\left(T - T_\infty\right) + \sigma\varepsilon\left(T^4 - T_\infty^4\right);\ t > 0;\ 0 < x < H;\ 0 < y < L; \tag{5}$$

and the boundary condition of the concave surface:

$$-k\frac{\partial T}{\partial x} = -k\frac{\partial T}{\partial y} = h\left(T - T_\infty\right) + \varepsilon(\theta)(G - e_b(T)) \tag{6}$$

The y direction is chosen tangential to the arc and the X direction longitudinal with front faces of the 3D tube section perpendicular on the Y axis. As we see in Eq. (5) and (6) some of the boundary conditions are non-linear homogeneous differential equations. Here T defines the temperature in Kelvin, α is the thermal diffusivity in $(\frac{\mathrm{m}^2}{\mathrm{s}})$, k is the thermal conductivity in $(\mathrm{W}((\mathrm{m} \cdot \mathrm{K})))$, L, H and d are respectively the arc length, the height and thickness of the tube section in (m), h is the coefficient of convection in (W((m2.K))), σ is the Stephan-Boltzmann constant, Γ is the reflectivity coefficient and ε is the emissivity in function of θ, the angle between the ray and the normal vector (°). G and J are respectively the incoming and outgoing radiative flux in $(\mathrm{W/m}^2)$. The coefficient of convection is calculated by the software according to [21] from the knowledge that it is a vertical plate considering natural convection with a vertical length of the plate equal to the height H of the tube section. The ambient temperature $mathrmT_\infty = 295\mathrm{K}$.

The radiation and irradiation are calculated using the Monte Carlo ray tracing methodology whereby a fixed amount of 2000 rays are emitted from each concave surface element to calculate the local irradiation, symbolized by G_m. Besides, part of the rays are emitted towards the environment. This is calculated by the ambient radiation field factor F_∞ and with n as the refraction index of the solid body. The outgoing radiative flux for each element of the model is calculated by:

$$J = \Gamma G + \varepsilon(\theta) e_b(T) \tag{7}$$

whereby the power radiated across all wavelengths and the incoming radiative flux is defined by:

$$e_b(T) = n^2 \sigma T^4 \text{ and } G = G_m(J) + F_\infty e_b(T_\infty);\ t > 0;\ 0 < x; y < L \tag{8}$$

3. Results and discussion

In the next section we will present and discuss the results from the FE updating of the unknown parameters for the directional emissivity. We will start with a discussion of the experimental results, proceed with the numerical results and end with the results after the model updating and a discussion of the obtained accuracy.

3.1. Experimental results

The experimental measurements of the tube section demonstrate a clear difference between the convex and concave surface with an equal temperature. An equal temperature perpendicular to the camera is measured as is shown in Figure 3. We can further see that the concave surface has an increased measured temperature at the sides which are oriented towards each other due to the directional emissivity.

We can explain the measured temperature rise between 5 and approximately 25 mm on the diametrical distance as a result of the directional emissivity, furthermore we can explain the temperature drift between 70 and 90 mm. If we look closely we can see a local temperature peak in the middle. As this is the location of the camera we suppose that this increase is caused by the external reflection of the camera body and should be neglected.

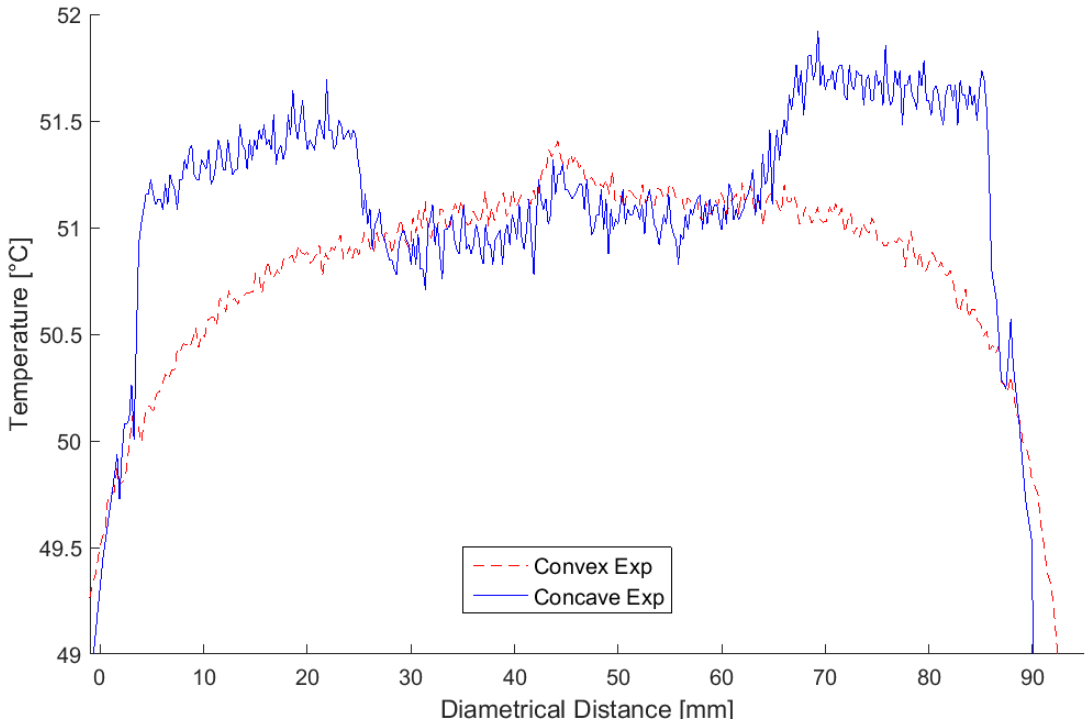

Figure 3: The measured temperature at the concave and convex horizontal mid-arc of a homogeneous cooling surface at $51°C$.

As the tube section can be considered as a perfect cylindrical face, we can use the assumed reflection of the camera in the middle as reference point to map the concave and convex plot. We need to remark an unexpected fast transition between the elevated temperature at the sides and the decreasing profile in the middle of the concave surface. It is assumed that this a result of a different surface roughness of the steel below the coating. This will be further discussed in section 3.3 but it should be remarked that this means that the acrylic coating is semi-transparent for the IR spectrum investigated, which means that the sub-level structure is inspected.

3.2. Numerical results

From the numerical simulations we can see the influence of the directional emissivity on the concave surface. The numerical results are performed in conformity with the setup as explained in 2.3. By using the Monte Carlo ray tracing technique the results show the increased received radiation at the sides relative to the middle of the tube section. We are only interested in the data of the mid-plane of the concave surface. The convex surface is neglected in the numerical simulation as the numerical calculations deliver temperature results for the surfaces perpendicular to the element. A plot of the numerical results is shown in Figure 4. We need to remark the difference between the experimental and the numerical results of the concave surface. We will focus further on this in the next subsection.

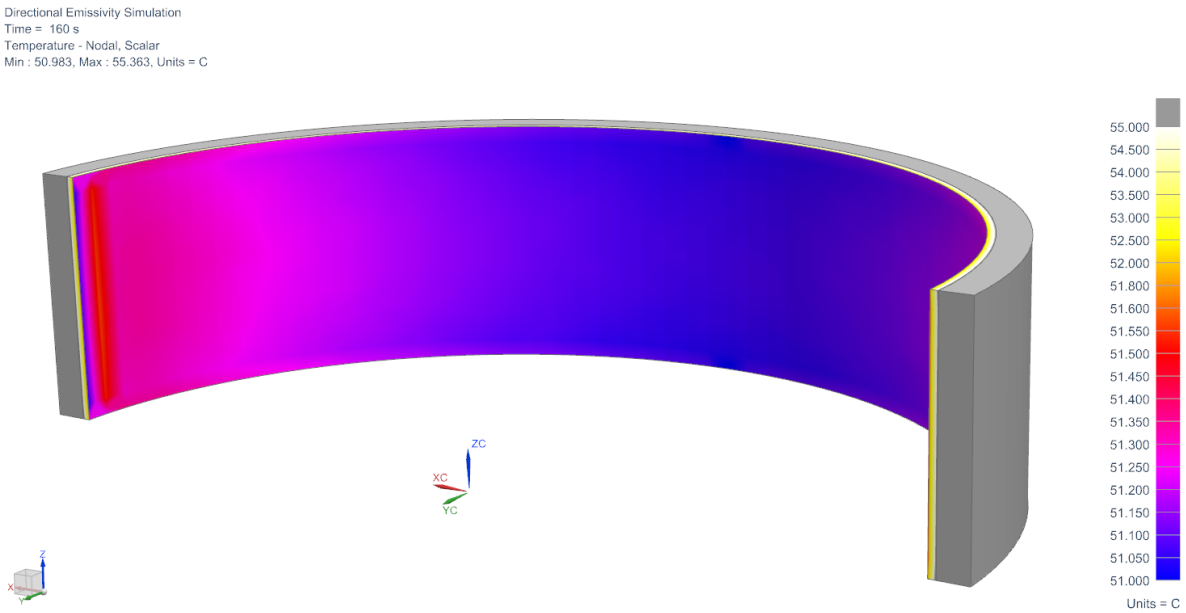

Figure 4: Temperature distribution obtained from the finite element model results of the concave surface. As expected, the numerical model shows the same temperature distribution with a higher temperature at the sides and a lower temperature in the middle.

3.3. Discussion

The temperature profile of the side sections of the steel tube section is different for the experimental and numerical data as shown in Figure 5. The curvature follows the same profile in the middle section, but at the two side sections the experimental curve is flattened while the numerical model predicts a continuous increasing temperature. We found a possible explanation by validating the results with the measurements on the nylon tube section which is an homogeneous polymer. This is shown in Figure 6 and here we find a better match between the numerical and experimental data. From this it can be concluded that the updated FE model matches the experimental data for non-reflecting polymer materials. The geometrical and experimental conditions of both tube sections (nylon and steel) are exactly the same and the estimated emissivities have the same amplitude due to the acrylic coating. Now, it can be concluded that the major difference between the two results is the surface treatment of the steel tube section. Therefore, we investigated the surface structure of the tube using a Quanta scanning electron microscope (SEM) in a second stage to understand the different behaviours of the two experimental cases. We inspected two samples of the steel tube without the acrylic coating, one from the middle section and one from the side at the location of the discontinuous profile. In Figure 7 we can see that the surface structure of the two zones differs. In the middle of the tube we have a microscopic homogeneous rough surface (Figure 7a) and at the side of the tube the surface is harder with less scratches. The main scratch direction at the sides follows the direction of the tube. This is the z direction in the numerical analysis plot of Figure 4. If

we compare the atomic substance distribution we remark a high oxide percentage which is higher for the side section than for the middle section. This suggests a remaining oxidized layer between the acrylic coating and the steel tube. This explains the difference between the middle and side section and shows that it is possible to detect the oxidized layer.

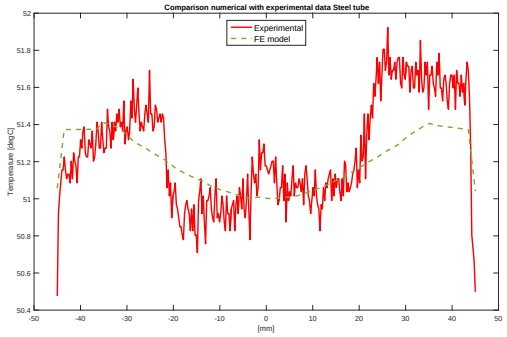

Figure 5: Comparison of the numerical data with the experimental data of the Steel tube section.

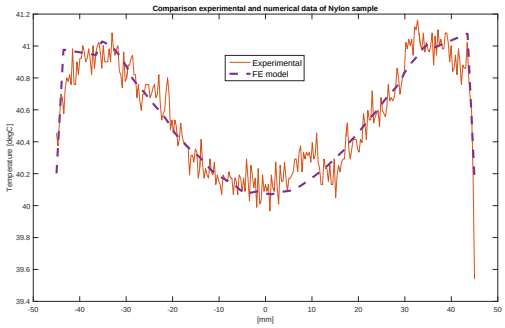

Figure 6: Comparison of the numerical data with the experimental data of the Nylon tube section.

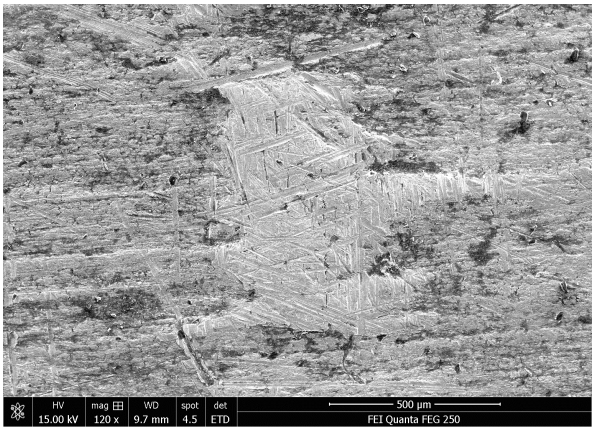

(a) The surface at the middle of the tube with the bright spot at the left and a homogeneous diffuse rough surface.

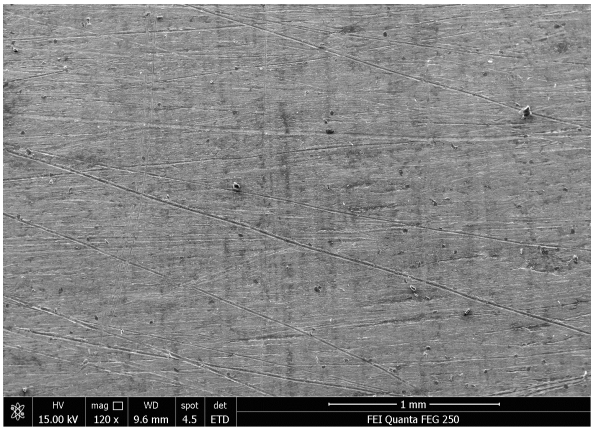

(b) surface at the side of the tube with smoother surface and in general one main scratch direction.

Figure 7: Comparison of the surfaces at the middle of the tube and at the side.

4. Conclusions

This paper has investigated the accuracy of numerical modelling of directional emissivity. Firstly, it is shown experimentally that temperature differences occur in complex shaped surfaces due to directional emissivity. Conform to literature it is shown that acrylic coatings are semi-transparent for IR radiation which results in an influence of the sub-level surface roughness on the measured temperatures. Secondly, numerical simulations are used to

estimate the directional emissivity. For the nylon model the numerical simulation gives an accurate prediction of the experimental measurements. For the steel tube the correlation is more complex. Due to a local sub-level remaining oxidized layer shown by scanning electron microscopy, the reradiating surfaces have a different surface roughness than the mid-plane which delivers an offset for the side regions. Returning to the hypothesis posed at the beginning of this article, it is now possible to state that it is possible to estimate the errors of thermal imaging testing of complex shapes using a numerical model. This methodology can be used to accurately predict and optimize thermography experiments of complex shaped structures using numerical models as performed on flat test samples in [22]. Further work needs to be done to evaluate the accuracy of the updating routine for multiple curved realistic samples in industrial conditions.

Acknowledgements

We would like to thank Christof Vandevelde, consultant of the software Siemens NX for his software support and the EMAT research group to provide support to this research with the use of their FEI Quanta Scanning Electron Microscope and their expertise. This research has been funded by the University of Antwerp and the Institute for the Promotion of Innovation by Science and Technology in Flanders (IWT) by the support to the TETRA project 'Smart data clouds' with project number 140336. Furthermore, the research leading to these results has received funding from Industrial Research Fund FWO Krediet aan navorsers 1.5.240.13N. The authors also acknowledge the Flemish government (GOA-Optimech) and the research councils of the Vrije Universiteit Brussel (OZR) and University of Antwerp (fti-OZC) for their funding.

Bibliography

[1] X. Maldague, Theory and practice of infrared thermography for nondestructive testing, Wiley, Quebec, 2001.

[2] M. Krishnapillai, R. Jones, I. Marshall, M. Bannister, N. Rajic, Thermography as a tool for damage assessment, Composite Structures 67 (2) (2005) 149–155. doi:10.1016/j.compstruct.2004.09.015.

[3] M. Vollmer, K. Möllmann, Infrared thermal imaging: fundamentals, research and applications, Wiley-VCH, Berlin, 2010.

[4] V. Vavilov, Thermal NDT Historical milestones , state -of-the-art and trends, in: QIRT2014 Conférence, Qirt, Bordeaux, 2014, p. 1.

[5] K. Kanayama, Apparent Directional Emittances of Random Rough surfaces of metals and nonmetals, Kitami Institute of technology journal.

[6] F. Ghmari, T. Ghbara, M. Laroche, R. Carminati, J. J. Greffet, Influence of microroughness on emissivity, Journal of Applied Physics 96 (2004) 2656–2664. doi:10.1063/1.1776634.

[7] K. E. Torrance, E. M. Sparrow, Biangular Reflectance of an Electric Nonconductor as a Function of Wavelength and Surface Roughness, Journal of Heat Transfer 87 (2) (1965) 283–292.

[8] H. F. Nelson, R. Goulard, Reflection from a periodic dielectric surface., JOSA (1967) 769–770.

[9] R. Birkebak, E. Eckert, Effects of roughness of metal surfaces on angular distribution of monochromatic reflected radiation., Journal of Heat Transfer 87 (1) (1965) 85–&.

[10] V. Rammohan Rao, V. M. K. Sastri, Efficient evaluation of diffuse view factors for radiation, International Journal of Heat and Mass Transfer 39 (6) (1996) 1281–1286. doi:10.1016/0017-9310(95)00203-0.

[11] a. Sentenac, H. Giovannini, M. Saillard, Scattering from rough inhomogeneous media: splitting of surface and volume scattering., Journal of the Optical Society of America. A, Optics, image science, and vision 19 (4) (2002) 727–736. doi:10.1364/JOSAA.19.000727.

[12] H. Brockmann, The use of generalized configuration factors for calculating the radiant interchange between nondiffuse surfaces, International Journal of Heat and Mass Transfer 40 (18) (1997) 4473–4486. doi:10.1016/S0017-9310(97)00071-9.

[13] S. Petrocelli, T. Sentenac, Y. L. Maoult, 3D Thermal Imaging : An approach towards true field temperature measurement, in: QIRT2014 Conférence, Qirt, Bordeaux, 2014, p. 10.

[14] L. Salvi, L. Vitali, D. Fustinoni, P. Gramazio, A. Niro, P. Milano, V. Lambruschini, Preliminary Pulsed Phase Thermography analysis on cylindrical geometry, in: QIRT2014 Conférence, Qirt, Bordeaux, 2014, p. 10.

[15] S. Deheng, Z. Fenghui, Z. Zunlue, S. Jinfeng, Modeling the effect of surface oxidation on the normal spectral emissivity of steel 316L at 1.5 μm over the temperatures ranging from 800 to 1100 K in air, Infrared Physics & Technology 71 (2015) 370–377.

[16] A. Araújo, S. Silvano, N. Martins, Monte Carlo uncertainty simulation of surface emissivity at ambient temperature obtained by dual spectral infrared radiometry, Infrared Physics & Technology 67 (2014) 131–137. doi:10.1016/j.infrared.2014.07.018.

[17] A. V. Prokhorov, S. N. Mekhontsev, L. M. Hanssen, Emissivity modeling of thermal radiation sources with concentric grooves, High Temperatures - High Pressures 35-36 (2003) 199–207. doi:10.1068/htjr093.

[18] Granta, PMMA, material datasheet (2013).

[19] R. K. Nagle, E. B. Saff, A. D. Snider, Fundamentals of Differential Equations and Boundary Value Problems, Pearson education, 2012.

[20] (Comsol Multiphysics), Comsol Documentation (2015).

[21] T. L. Bergman, A. S. Lavine, F. P. Incropera, D. P. DeWitt, Fundamentals of Heat and Mass Transfer, 2011.
URL http://books.google.com/books?id=vvyIoXEywMoC&pgis=1

[22] J. Peeters, G. Arroud, B. Ribbens, J. Dirckx, G. Steenackers, Updating a finite element model to the real experimental setup by thermographic measurements and adaptive regression optimization, Mechanical Systems and Signal Processing 64-65 (2015) 428–440. doi:10.1016/j.ymssp.2015.04.010.